Scripta Materialia 143 (2018) 86–89

Contents lists available at ScienceDirect

Scripta Materialia

journal homepage: www.elsevier.com/locate/scriptamat

Regular article

Structural connection between gallium crystals and near-T_m liquids under ambient pressure

F. Zhang [a,*], Y. Sun [a], X.D. Wang [b], Q.P. Cao [b], J.Z. Jiang [b], C.Z. Wang [a], K.M. Ho [a,c,d]

[a] Ames Laboratory, US Department of Energy, Ames, IA 50011, USA
[b] International Center for New-Structured Materials (ICNSM), Laboratory of New-Structured Materials, State Key Laboratory of Silicon Materials, School of Materials Science and Engineering, Zhejiang University, Hangzhou, 310027, People's Republic of China
[c] Department of Physics, Iowa State University, Ames, IA 50011, USA
[d] Hefei National Laboratory for Physical Sciences at the Microscale and Department of Physics, University of Science and Technology of China, Hefei, Anhui 230026, People's Republic of China

ARTICLE INFO

Article history:
Received 6 June 2017
Received in revised form 23 August 2017
Accepted 12 September 2017

Keywords:
Liquids
Short-range ordering
Crystallization
Genetic algorithm
Molecular dynamics

ABSTRACT

We study the short-range structural order in liquid gallium prepared by ab initio molecular dynamics simulations. We found that at 400 K, which is close to the melting point (Tm) of Ga, the dominant motif in the liquid phase is identical to that in the stable solid phase Ga-I. Strong directional bonding in this motif prevents it from nucleation in the liquid phase. Meanwhile, a newly identified motif, topologically distinct from yet related to those in β-Ga and Ga-III phases, is also abundant in Ga liquid. This new motif could serve as precursors for β-Ga or Ga-III during crystallization.

Published by Elsevier Ltd on behalf of Acta Materialia Inc.

Gallium is an element that exhibits profound complexity in both liquid and crystalline phases. Under ambient pressure, Ga has a stable orthorhombic phase Ga-I [1] that has hybrid covalent and metallic bonding characters according to *ab initio* calculations [2,3]. Ga-I has a very low melting temperature (T_m) of 303 K, and the liquid phase shows anomalous features in the structure factor, which can also be attributed to partial covalent bonding [4–6]. When Ga liquid is cooled below T_m, it does not necessarily crystallize into the stable Ga-I phase; instead, a series of metastable phases can be accessed [7]. In particular, highly supercooled Ga liquid droplets have a clear tendency to form a triclinic metastable β-Ga phase [8] before finally transforming into Ga-I [9]. In our current *ab initio* molecular dynamics (AIMD) simulations, under an ultrafast cooling rate of 3.3×10^{15} K/s, the liquid sample crystallizes into the body-centered tetragonal (bct) Ga-III phase, which is metastable at ambient pressure and can be stabilized at high pressure and high temperature [7].

Knowledge about the liquid structure is necessary to understand the complex phase selection. While apparently lacking long-range translational symmetry, liquids have clear short-range order (SRO), which is usually characterized by typical local clusters up to the first atomic shell. Such structural order can have a large impact on crystallization or vitrification processes upon fast quenching [10–12]. Earlier work used the Honeycutt-Anderson (HA) common-neighbor analysis [13] to study the ordering in Ga liquids [5,14]. However, since HA index only reveals a fragment of a local cluster [15], such analysis can hardly give a complete picture of the dominant SRO in the liquid phase. Recently, it was demonstrated that typical undercooled metallic liquids or glasses share the same SRO, which was called "crystal genes", with a series of crystalline structures in glass forming binary alloys Cu-Zr and Al-Sm [16]. It is intriguing to examine whether the concept of crystal genes persists in the single-elemental Ga liquid with complicated chemical bonding.

Since the crystal genes may not exist in known crystalline phases of Ga, we performed a systematic genetic-algorithm (GA) search [17,18] for more low-energy crystalline structures containing up to 50 atoms per unit cell. To facilitate the search, a semi-empirical Tersoff potential [19] was used for energy calculations during the search. Then, 100 structures with the lowest Tersoff energy in the converged GA pool were collected for relaxations using more accurate density-functional theory (DFT), as implemented in the VASP code [20]. The projected augmented-wave (PAW) method [21] is used to describe the electron-ion interaction, and the generalized gradient approximation (GGA) in the Predew-Burke-Ernzerhof (PBE) form [22] is employed for the exchange-correlation energy functional. An energy cutoff of 168.35 eV was used for the plane-wave basis set. A dense *k*-point mesh generated using the automatic scheme [23] the length parameter $l = 25$ Å, to guarantee the *k*-points are evenly distributed in the Brillouin zone.

Our GA search successfully identified the Ga-I as the ground state phase at 0 K and under ambient pressure. The next two lowest-energy

* Corresponding author.
E-mail address: fzhang@ameslab.gov (F. Zhang).

http://dx.doi.org/10.1016/j.scriptamat.2017.09.019
1359-6462/Published by Elsevier Ltd on behalf of Acta Materialia Inc.

structures in the GA pool are Ga-III and β-Ga, respectively. Other structures in the GA pool have not been observed in experiments. We then analyze the clusters surrounding each Ga atom up to the first atomic shell. Interestingly, all the clusters collected from the 10 lowest-energy structures can be classified by only 4 different motifs, suggesting energetic stability of these 4 motifs. The atomic configurations of these 4 motifs are shown in Fig. 1 and their presence in the l0 lowest-energy structures in the GA search is summarized in Table 1. In Fig. 1, M1 and M2 have a low coordination number of 7, as compared with 12 in close-packing fcc or hcp structures. There are dimer-like Ga—Ga bonds with short bond-lengths of ~2.5 Å in both M1 and M2 motifs, showing significant covalent bonding characters. The coordination number is increased to 8 and 12 in M3 and M4, respectively. The minimal bond length is also increased to 2.80 Å and 2.95 Å in M3 and M4, respectively. These facts indicate increasing metallic bonding characters in M3 and M4. Especially, the ideal M4 motif, collected from the Ga-III phase [7], has a bct structure with $c/a = 1.49$ in our DFT calculations. Ga-III can be considered as a deformed fcc phase, since fcc can also be viewed as bct with $c/a = \sqrt{2}$. Indeed, a phase transition from bct (Ga-III) to fcc (Ga-IV) can occur under high pressure of ~150 GPa [24]. Motifs M2–M4 also share a similar "boat"-like substructure, as shown by the red atoms in Fig. 1. However, due to the different bond lengths and shape of the "boat", together with the differences in other parts as highlighted by the green atoms in Fig. 1, these three motifs are clearly distinguishable. Later, we will demonstrate that the relation in these motifs might play an important role in phase selection during crystallization of Ga liquids.

We have performed AIMD simulations to prepare the liquid sample. In AIMD, we used Nosé-Hoover thermostat [25] to control the temperature, and a time interval of 3 fs to integrate Newton's equations of motion. A smaller energy cutoff of 134.68 eV, compared with structural relaxation, was used for the plane-wave basis in AIMD to accelerate the calculation. Only the Γ point was used to sample the Brillouin zone since the simulation box was sufficiently large. A cubic box with periodic boundary conditions, containing 216 Ga atoms, was fully melted at 2000 K to remove the crystalline symmetry and reach thermal equilibrium, followed by step-wise cooling to 400 K with a rate of 0.1 K per

Table 1
Energy and motifs of 10 lowest-energy structures identified in Ga search. Energy is referenced to the ground state Ga-I.

No.	1 (Ga-I)	2 (Ga-III)	3 (β-Ga)	4	5
Energy (meV/atom)	0	1.6	6.3	8.0	9.2
Motifs	M1	M4	M3	M3	M4
No.	6	7	8	9	10
Energy (meV/atom)	9.8	11.2	13.3	16.8	27.1
Motifs	M3	M3	M4	M1, M2	M2, M3

MD step. The internal pressure was maintained almost zero by adjusting the box size during the cooling process. After that, the sample was annealed at 400 K for additional 12,000 steps. In a recent publication, we have reported that the AIMD samples clearly display liquid behavior at $T = 400$ K and above with a profound change of the liquid structure at around 1000 K [26]. Here, we focus on a near-T_m temperature: 400 K.

Then, the clusters extracted from the liquid sample are compared with the GA-identified motifs in Fig. 1, following a cluster-alignment method [15]. An alignment score, quantitatively describing how an as-extracted cluster deviates from a template motif, is defined as

$$f = \min_{0.80 \le \alpha \le 1.2} \left(\frac{1}{N} \sum_{i=1}^{N} \frac{(\mathbf{r}_{ic} - \alpha \mathbf{r}_{it})^2}{(\alpha \mathbf{r}_{it})^2} \right)^{1/2}, \quad (1)$$

where N is the number of atoms in the template motif; $\mathbf{r}_{ic}$ and $\mathbf{r}_{it}$ are the atom positions in the cluster and template after the alignment, respectively; and α is a coeffient to adapt the template's bond length in order to achieve an optimal alignment. The smaller the alignment score is, the more similar the cluster is to the template. We show in Fig. 2(a) the distribution of the alignment score obtained by aligning the clusters in the AIMD sample at $T = 400$ K with all the cluster motifs given in Fig. 1, from which one can see that the popularity of M1-M4 decreases in the liquid sample as the peak position moves to larger values. For comparison purpose, we also show in Fig. 1(a) the score distribution for aligning clusters in Ga liquids with the icosahedron (ICO) motif, one of the most commonly seen structural order in liquids [27], *e.g.*, in Al liquids that belongs to the same group as Ga in the periodic table [15]. In contrast, the icosahedron motif is the least favored among all examined

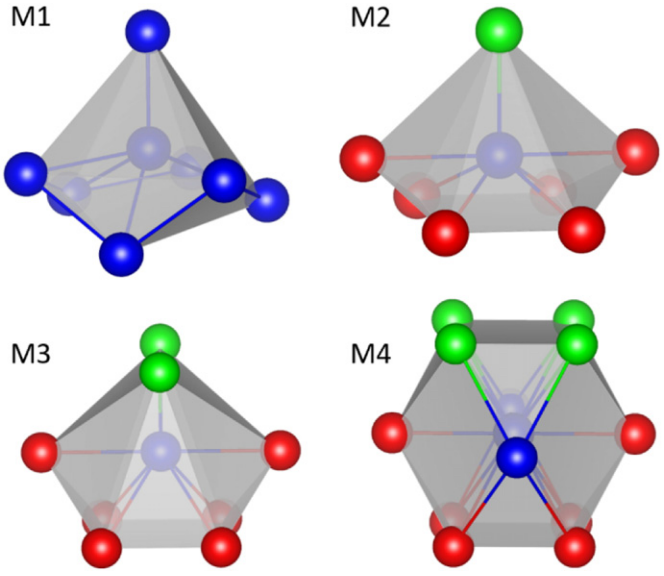

Fig. 1. Most popular first-shell cluster motifs in low-energy structures found by a GA search. M1 exists in Ga-I, M3 in β-Ga, and M4 in Ga III. M2 is not seen in previously known Ga phases. Atoms of all colors represent Ga. In M2, M3 and M4, red atoms show a similar "boat-like" substructure, while the green atoms highlight the difference in these motifs.

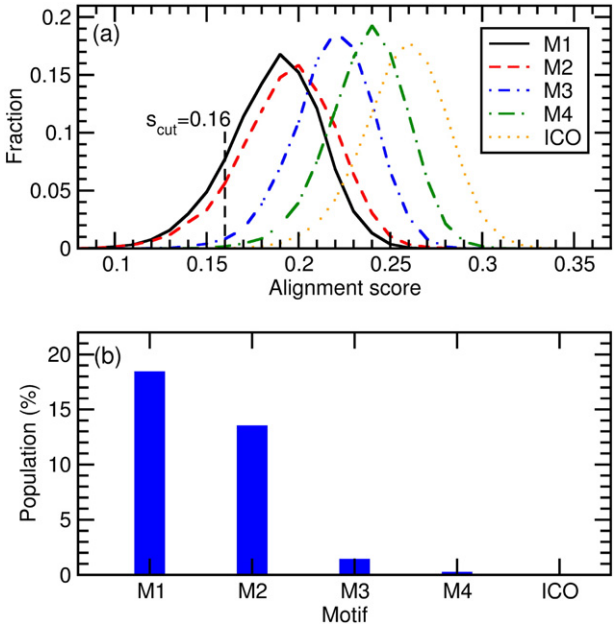

Fig. 2. (a) Distribution of the alignment score and (b) population for clusters extracted from the AIMD sample at $T = 400$ K aligned with the cluster motifs given in Fig. 1, as well as the icosahedron motif.

motifs in Ga liquids at 400 K, which, again, demonstrates significant differences in chemical bonding in the liquid Ga and some of the simple metals such as Al. A cutoff vaue for the alignment score s_{cut} was introduced to quantitatively determine the population of each motif, defined as the percentage of the clusters in the liquid sample with alignment score smaller than s_{cut}, when aligned with the corresponding motif. Here, s_{cut} was chosen to be 0.16 as denoted in Fig. 2(a), but our results do not depend on any specific choice of s_{cut}. Fig. 2(b) gives the population of each motif. The M1 motif, which is the characteristic cluster in the stable Ga-I phase under ambient pressure (see Table 1), has the largest population of 18.4%, demonstrating a clear similarity between the Ga-I phase and near-T_m liquid phase under ambient pressure. Because the directional covalent bonds in M1 make it hard to pack into a periodic network, Ga liquids can sustain a large population of M1 motifs without nucleation near the melting point. Another typical motif with significant molecular bonding characters M2 also has a large population (13.5%) in the liquid sample at 400 K, as shown in Fig. 2(b). On the other hand, M3 and M4, which represent crystal phases with strong stability β-Ga, and Ga-III, respectively, are significantly less favored than M1 and M2. This result is reasonable since the stronger metallic bonding in M3 and M4 make them more prone to nucleation, and thus cannot survive in equilibrium liquid state. The icosahedral order is essentially non-existent in liquid Ga.

When Ga liquid is cooled below T_m under ambient pressure, it does not necessarily nucleate into the thermodynamically stable phase Ga-I; instead, several other phases can be formed including β-Ga. Interestingly, in our AIMD simulations, when the liquid sample was further cooled to 300 K, we observed the nucleation of Ga-III. Although the M1 motif is prevalent in Ga liquid, it might experience a large kinetic barrier to pack these M1-type clusters into the Ga-I phase due to the strong covalent bonding in M1. On the other hand, considering the connection between the M2 motif and the motifs seen in β-Ga and Ga-III (M3 and M4, respectively) as illustrated in Fig. 1, we believe that the M2-type clusters, which also has a significant population in the liquid, can serve as precursors for assembling M3- and M4-type clusters during crystallization in β-Ga and Ga-III phases, respectively.

To test this hypothesis, we instantly quench the sample from $T =$ 400 K to 300 K. Then, the sample was held at 300 K for about 30 ps. Fig. 3 shows the change of the total potential energy (the kinetic energy is not included), as well as the population of the relevant M1, M2 and M4 type clusters, during the annealing process. Initially, the potential energy decreases slowly following the instant quench due to the relaxation of the undercooled liquid. However, at t = ~4.8 ps, there is a sudden increase of the speed at which the potential energy drops, signaling the onset of the crystallization process. The crystallization completes at t = ~15 ps. During this process, the population for both M1 and M2 type clusters decreases, while that of the M4 type cluster dramatically increases, confirming that the liquid Ga transforms into the Ga-III phase. The M3 motif is not shown since it does not have an appreciable population during the entire process, indicating β-Ga is not involved. More importantly, as denoted by the red dashed line in Fig. 3, the M4 population changes almost at the same time as the M2 population, which also well-coincides with the onset of the fast drop of the potential energy. On the other hand, the decrease of M1 population occurs at a notably later time, as shown by the black dashed line in Fig. 3. This clearly indicates that the crystallization was initiated by converting some M2-type clusters to M4, which is topologically close to M2.

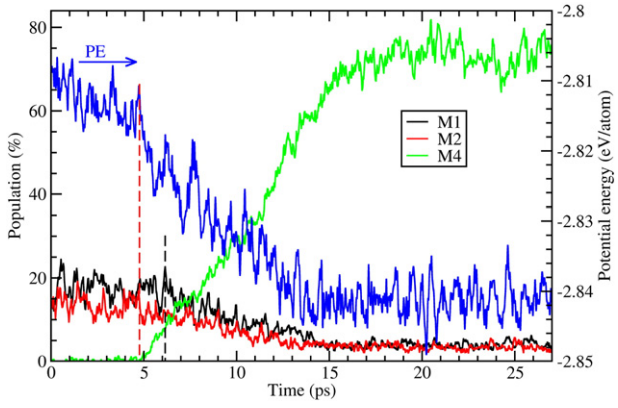

Fig. 3. The change of population of M1, M2 and M4 type clusters, as well as the potential energy (right axis) as a function of annealing time for Ga at $T = 300$ K. The dashed red line denotes the simultaneous onset of increase of M4 population, decrease of M2 population, and the sudden increase of the speed at which the potential energy drops. The dashed black line denotes the onset of the decrease of M1 population.

While we did not directly observe the crystallization of β-Ga in our AIMD simulations, we believe in principle, a similar scenario can apply to β-Ga as well under different processing conditions. Since both β-Ga and Ga-III display almost pure metallic bonding [2,3], crystallization in these two phases is characterized by monoatomic packing, which in general is a fast process. Of course, the structural connection between the liquid and solid phases, as discussed in the above, can only be part of reasons for the actual phase selection during crystallization. Other factors include the thermodynamic driving force, atomic diffusivity, *etc.*, which are beyond the scope of the current study.

In summary, we establish the structural connection, or crystal genes, between Ga crystals and the liquid phases near the melting point. *Ab initio* molecular dynamics simulations were performed to create the liquid sample. We found that Ga liquid share the most dominant SRO with the stable Ga-I phase. Strong directional covalent bonds in this SRO make it difficult for Ga liquid to crystallize in the Ga-I phase. In addition, we identified a new motif from genetic algorithm search. This motif is topologically distinct from yet related to those in β-Ga and Ga-III phases. A cluster alignment study found that the new motif is also abundant in Ga liquid at 400 K, and could serve as precursors for β-Ga or Ga-III phases during crystallization. It should also be noted that while we identified two dominant motifs M1 and M2, there is still a large fraction of clusters in the liquid sample that failed to be characterized by any of the populous motifs we found in crystalline phases. Therefore, continuous work is desired in order to achieve a complete understanding of the amorphous liquid structure, which remains a significant challenge in materials science.

Work at Ames Laboratory was supported by the US Department of Energy, Basic Energy Sciences, Division of Materials Science and Engineering, under Contract No. DE-AC02-07CH11358, including a grant of computer time at the National Energy Research Supercomputing Center (NERSC) in Berkeley, CA. The AIMD simulations were performed in Zhejiang University, with financial supports from the National Natural Science Foundation (No. 51371157, U1432105, U1432110, U1532115, 51,671,170 and 51,671,169), the National Key Research and Development Program of China (No. 2016YFB0701203 and 2016YFB0700201), the Natural Science Foundation of Zhejiang Province (No. Z1110196 and Y4110192), and the Fundamental Research Funds for the Central Universities. The computer resources at National Supercomputer Centers in Tianjin and Guangzhou are also gratefully acknowledged. K.M.H. acknowledges support from USTC Qian-Ren B (1000-Talents Program B) fund.

References

[1] B.D. Sharma, J. Donohue, Z. Kristsllogr. - Cryst. Mater. 117 (1962) 293–300.
[2] X.G. Gong, G.L. Chiarotti, M. Parrinello, E. Tosatti, Phys. Rev. B 43 (1991) 14277–14280.
[3] M. Bernasconi, G.L. Chiarotti, E. Tosatti, Phys. Rev. B 52 (1995) 9988–9998.
[4] X.G. Gong, G.L. Chiarotti, M. Parrinello, E. Tosatti, Europhys. Lett. 21 (1993) 469–475.
[5] S.F. Tsay, S. Wang, Phys. Rev. B. 50 (1994) 108–112.
[6] K.H. Tsai, T.M. Wu, S.F. Tsay, J. Chem. Phys. 132 (2010) 034502.
[7] L. Bosio, J. Chem. Phys. 68 (1978) 1221–1223.
[8] L. Bosio, A. Defrain, H. Curien, A. Rimsky, Acta Crystallogr. Sect. B: Struct. Crystallogr. Cryst. Chem. 25 (1969) 995.

[9] L. Bosio, C.G. Windsor, Phys. Rev. Lett. 35 (1975) 1652–1655.
[10] L. Huang, C.Z. Wang, K.M. Ho, Phys. Rev. B 83 (2011) 184103.
[11] H.Z. Fang, X. Hui, G.L. Chen, R. Öttking, Y.H. Liu, J.A. Schaefer, Z.K. Liu, Comput. Mater. Sci. 43 (2008) 1123–1129.
[12] D.D. Wen, P. Peng, Y.Q. Jiang, R.S. Liu, J. Non-Cryst. Solids 378 (2013) 61–70.
[13] J.D. Honeycutt, H.C. Andersen, J. Phys. Chem. 91 (1987) 4950–4963.
[14] S.F. Tsay, Phys. Rev. B 50 (1994) 103–107.
[15] X.W. Fang, C.Z. Wang, Y.X. Yao, Z.J. Ding, K.M. Ho, Phys. Rev. B 82 (2010) 184204.
[16] Y. Sun, F. Zhang, Z. Ye, Y. Zhang, X. Fang, Z. Ding, C.-Z. Wang, M.I. Mendelev, R.T. Ott, M.J. Kramer, K.-M. Ho, Sci. Rep. 6 (2016) 23734.
[17] D.M. Deaven, K.M. Ho, Phys. Rev. Lett. 75 (1995) 288.
[18] S.Q. Wu, M. Ji, C.Z. Wang, M.C. Nguyen, X. Zhao, K. Umemoto, R.M. Wentzcovitch, K.M. Ho, J. Phys. Condens. Matter 26 (2014) 35402.
[19] J. Nord, K. Albe, P. Erhart, K. Nordlund, J. Phys. Condens. Matter 15 (2003) 5649–5662.
[20] G. Kresse, J. Furthmüller, Comput. Mater. Sci. 6 (1996) 15–50.
[21] P.E. Blochl, Phys. Rev. B 50 (1994) 17953.
[22] J.P. Perdew, K. Burke, M. Ernzerhof, Phys. Rev. Lett. 77 (1996) 3865–3868.
[23] See VASP manual at https://cms.mpi.univie.ac.at/vasp/vasp/Automatic_k_mesh_generation.html.
[24] T. Kenichi, K. Kazuaki, A. Masao, Phys. Rev. B Condens. Matter 58 (1998) 2482–2486.
[25] S. Nosé, J. Chem. Phys. 81 (1984) 511.
[26] L.H. Xiong, X.D. Wang, Q. Yu, H. Zhang, F. Zhang, Y. Sun, Q.P. Cao, H.L. Xie, T.Q. Xiao, D.X. Zhang, C.Z. Wang, K.M. Ho, Y. Ren, J.Z. Jiang, Acta Mater. 128 (2017) 304–312.
[27] F.C. Frank, Proc. R. Soc. Lond. A. Math. Phys. Sci. 215 (1952) 43–46.